Polyhedron 52 (2013) 170–182

Contents lists available at SciVerse ScienceDirect

Polyhedron

journal homepage: www.elsevier.com/locate/poly

A study of acetylene and acetylide carbonyl and diphosphine substituted ruthenium trinuclear clusters: Synthesis and structural characterization

Micaela Hernández-Sandoval [a], Gloria Sánchez-Cabrera [a], María J. Rosales-Hoz [b], Marco A. Leyva [b], Verónica Salazar [a], José G. Alvarado-Rodríguez [a], Francisco J. Zuno-Cruz [a,*]

[a] Centro de Investigaciones Químicas, Universidad Autónoma del Estado de Hidalgo, Ciudad Universitaria, km 4.5 Carretera Pachuca–Tulancingo, Pachuca Hgo., 42184 México, Mexico
[b] Departamento de Química, Centro de Investigación y Estudios Avanzados del I.P.N., Apdo. Postal 14-740, 07000 México DF, Mexico

ARTICLE INFO

Article history:
Available online 23 October 2012

Dedicated to Alfred Werner on occasion of the 100th Anniversary of his Nobel prize in Chemistry.

Keywords:
Ruthenium
Clusters
Acetylene
Acetylides

ABSTRACT

The synthesis and structural characterization of the acetylene and acetylide carbonyl ruthenium clusters: $[Ru_3(CO)_9(\mu\text{-}CO)\{\mu_3\text{-}\eta^2\text{-}(//)\text{-}HC{\equiv}CR\}]$ [R = C_6H_4-4-CH_3 (**1a**), C_6H_3-2,5-$(CH_3)_2$ (**1b**), C_6H_2-2,4,5-$(CH_3)_3$ (**1c**), C_6H_4-4-^{t}Bu (**1d**), C_6H_4-4-COH (**1e**), C_6H_4-4-NH_2 (**1f**)] and $[Ru_3(CO)_9(\mu\text{-}H)\{\mu_3\text{-}\eta^2\text{-}(\perp)\text{-}C{\equiv}CR\}]$ [R = C_6H_4-4-CH_3 (**2a**), C_6H_3-2,5-$(CH_3)_2$ (**2b**), C_6H_2-2,4,5-$(CH_3)_3$ (**2c**), C_6H_4-4-^{t}Bu (**2d**), C_6H_4-4-COH (**2e**), C_6H_4-4-NH_2 (**2f**)] are described. Compounds **1a–f** were obtained under very mild conditions from the known $[Ru_3(CO)_{10}(NCMe)_2]$ activated cluster in the presence of the monosubstituted phenylacetylenes; in all cases, the alkynes are coordinated to the metallic fragment as acetylene groups in a μ_3-η^2 parallel fashion without breaking the $C_{(sp)}$–H bond of the triple bond. In solution compounds of the **1** series slowly transformed to the acetylide derivatives (**2**), where the acetylene group undergoes an oxidative addition and a rearrangement of the –C≡C– coordinated fragment to a μ_3-η^2 perpendicular coordination mode of the C–C axis by breaking the $C_{(sp)}$–H bond to give a hydride ligand in each case. The diphosphines substituted derivatives $[Ru_3(CO)_7(\mu\text{-diphosphine})(\mu\text{-}H)\{\mu_3\text{-}\eta^2\text{-}(\perp)\text{-}C{\equiv}CR\}]$ [diphosphine = dppe; R = C_6H_4-4-CH_3 (**3a**), C_6H_3-2,5-$(CH_3)_2$ (**3b**), C_6H_2-2,4,5-$(CH_3)_3$ (**3c**) and diphosphine = dfppe; R = C_6H_4-4-CH_3 (**4a**), C_6H_3-2,5-$(CH_3)_2$ (**4b**), C_6H_2-2,4,5-$(CH_3)_3$ (**4c**)] were obtained from the reaction of the $[Ru_3(CO)_{10}$(diphosphine)] cluster (diphosphine = dppe or dfppe) with the terminal alkyne, respectively. All compounds have been characterized in solution by infrared spectroscopy and multinuclear magnetic resonance. The solid state structures of the acetylide compounds **2b–d** and **3b** have been established by single crystal X-ray diffraction studies; the –C≡C– fragment was observed in a μ_3-η^2 perpendicular coordination mode.

1. Introduction

The metal cluster compounds containing terminal alkynes have showed a great stability as well as a wide versatility in reactivity; these features have prompted their continuous synthesis and structural studies. For example, it is well known that an organic group stabilizes the metal cluster framework, avoiding its possible fragmentation. A number of saturated triruthenium-alkynyl clusters of general formula $[Ru_3(CO)_{10}(\mu_3\text{-}\eta^2\text{-}RC{\equiv}CR)]$ or $[Ru_3(CO)_9(\mu\text{-}H)(\mu_3\text{-}\eta^2\text{-}C{\equiv}CR)]$ has been synthesized from the direct reaction of alkynes with $[Ru_3(CO)_{12}]$ [1–3], or by displacement of labile ligands by the alkyne in activated precursors, such as $[Ru_3(CO)_{10}(NCMe)_2]$ [4–6]. Several structural studies on terminal alkynes with dodecacarbonyltriruthenium or some activated derivatives have shown that the carbon–carbon triple bond adopts a variety of bonding modes keeping intact the carbon skeleton [1,3,7–10].

In the field of alkyne-substituted trimetallic clusters the most common structural arrangements found are those in which the –C≡C– group use to cap a delta cluster either in a μ_3-η^2-(//) parallel or μ_3-η^2-($\perp$) perpendicular coordination mode [1,7,8,10,11]. When a terminal alkyne R–C≡C–H is coordinated to trinuclear ruthenium cluster derivatives via an oxidative addition as a μ_3-η^2-($\perp$) acetylide, the products are generally stable; however, the variation in electronic properties of either the cluster or the R-substituent may change the bonding interactions and, therefore, the cluster stabilization. Other observed bonding modes include a less stable μ_3-η^2 parallel coordination mode of the alkyne, the 1,2-H migration to form a vinylidene (=C=CHR) group, or a mode of reactivity that involves the scission of the triple bond (C≡C) to yield two alkylidyne ligands coordinated in a μ_3-η-CR mode. [12,13].

Moreover, it has been proposed that most unstable μ_3-η^2-(//) coordination mode of the alkynes could be achieved by incorporation of diphosphines, as dppm, due to an enhanced back-bonding ability of the metal induced by the bidentate ligand [5,14,15], which can help in stabilizing the binding mode μ_3-η^2-(//) parallel of the alkyne.

* Corresponding author. Tel.: +52 771 7172000x2204, cell: +52 1771 1625212; fax: +52 771 7172000x6502.
E-mail address: fjzuno@uaeh.edu.mx (F.J. Zuno-Cruz).

0277-5387/$ - see front matter © 2012 Elsevier Ltd. All rights reserved.
http://dx.doi.org/10.1016/j.poly.2012.10.013

Herein we report the synthesis and structural characterization of one new series of μ_3-η^2 acetylene (**1a**–**f**) and three new series of μ_3-η^2 acetylide (**2a**–**f**, **3a**–**c** and **4a**–**c**) triruthenium clusters. All compounds were characterized in solution by infrared and ^{1}H, ^{13}C{^{1}H}, ^{31}P{^{1}H} and ^{19}F{^{1}H} NMR spectroscopy and by 2D-heteronuclear correlation experiments for the complete assignment of carbon atoms. The molecular structures of compounds **2b**–**d** and **3b** in the solid state were determined by single crystal X-ray diffraction studies.

2. Results and discussion

The activated cluster $[Ru_3(CO)_{10}(NCMe_3)_2]$ reacts with an excess of a given terminal alkyne RC≡CH at room temperature [R = C_6H_4-4-CH_3 (**a**), C_6H_3-2,5-$(CH_3)_2$ (**b**), C_6H_2-2,4,5-$(CH_3)_3$ (**c**), C_6H_4-4-^{t}Bu (**d**), C_6H_4-4-COH (**e**), C_6H_4-4-NH_2 (**f**)], Scheme 1; the reaction was monitored by color changes and corroborated by thin layer chromatography (tlc) observing the formation of two compounds in each reaction. The compounds were isolated by preparative tlc using a mixture of hexane:$CHCl_3$ (80:20 v/v). The major product obtained in the series was identified as the parallel acetylene cluster **1** of general formula $[Ru_3(CO)_9(\mu\text{-}CO)\{\mu_3\text{-}\eta^2\text{-}(//)\text{-}HC{\equiv}CR\}]$ in moderate yields (**1a**, 44%; **1b**, 47%; **1c**, 45%; **1d**, 44%; **1e**, 43%; **1f**, 28%); the minor compound corresponds to the perpendicular acetylide cluster **2** $[Ru_3(CO)_9(\mu\text{-}H)\{\mu_3\text{-}\eta^2\text{-}(\perp)\text{-}C{\equiv}CR\}]$ (**2a**, 19%; **2b**, 23%; **2c**, 21%; **2d**, 28%; **2e**, 17%; **2f**, 19%). The compounds **2a** and **f** have been previously reported [16,17]. It is noteworthy that in chloroform solution the series of clusters **1** rapidly convert to clusters **2** in less than 2 h at room temperature, indicating the low stability of the parallel derivatives. The transformation can also be performed even at 0 °C.

The infrared spectra of clusters **1** are very similar in the carbonyl region; all of them display bands in the region of terminal CO and one absorption band attributed to the bridging carbonyl ligand from 1830 to 1844 cm^{-1}. The series **2** display just one ν(CO) pattern in the terminal region, similar to those previously reported in similar clusters [7,16–18]. In the ^{1}H NMR spectra of series **1**, a signal at high frequencies was observed, with chemical shifts ranging from 8.75 to 8.36 ppm; these data are similar to those observed in is structural complexes $[Ru_3(CO)_9(\mu\text{-}CO)\{\mu_3\text{-}\eta^2\text{-}(//)\text{-}HC{\equiv}CR\}]$ (R = $SiMe_3$, 9.18; $SiPh_3$, 8.95; ^{t}Bu, 8.31; H, 8.59; COH, 9.18 ppm), which were assigned to the terminal hydrogen atoms of the parallel alkynes [6,18]. In the ^{1}H NMR spectra of series **2**, the hydride signals were observed at lower frequencies ranging from −20.36 to−20.61 ppm, observing a rough tendency accordingly to the substituents on the phenyl ring following the order c > b > f > d > a > e. These data indicate that the electronic density increment in the cluster produces δ displacements to higher frequencies. Table 1 shows the full assignment of ^{1}H and ^{13}C NMR for all signals belonging to the different aromatic rings in the series **1** and **2**.

The information obtained from the ^{13}C{^{1}H} NMR spectra of the alkynyl ligands coordinated in either a parallel or perpendicular mode allowed us to perform an analysis of the $\delta(C_\alpha) + \delta(C_\beta)$ addition and $\delta(C_\alpha) - \delta(C_\beta)$ subtraction of the α and β carbon chemical shifts, which have been proposed to be related to the total charge alteration in the C≡C triple bond and its polarization, respectively [7,18,19]. The $\delta(C_\alpha) + \delta(C_\beta)$ data of the free ligands, the parallel derivatives (**1a**–**f**), and the acetylide compounds (**2a**–**f**) span from 156.9 to 163.9, 308.3 to 329.1, and 254.4 to 258.2 ppm, respectively, indicating that, upon coordination, the largest change in charge occurs in the parallel derivatives, while these are reduced in the acetylide compounds. These evidence can be explained in terms of the alkynyl coordination mode; in a parallel mode the σ:σ:π interactions of the C≡C fragment with the metal core produce the largest alteration in charge, while the change in coordination, due to the breaking the C–H bond by the σ:π:π interactions,

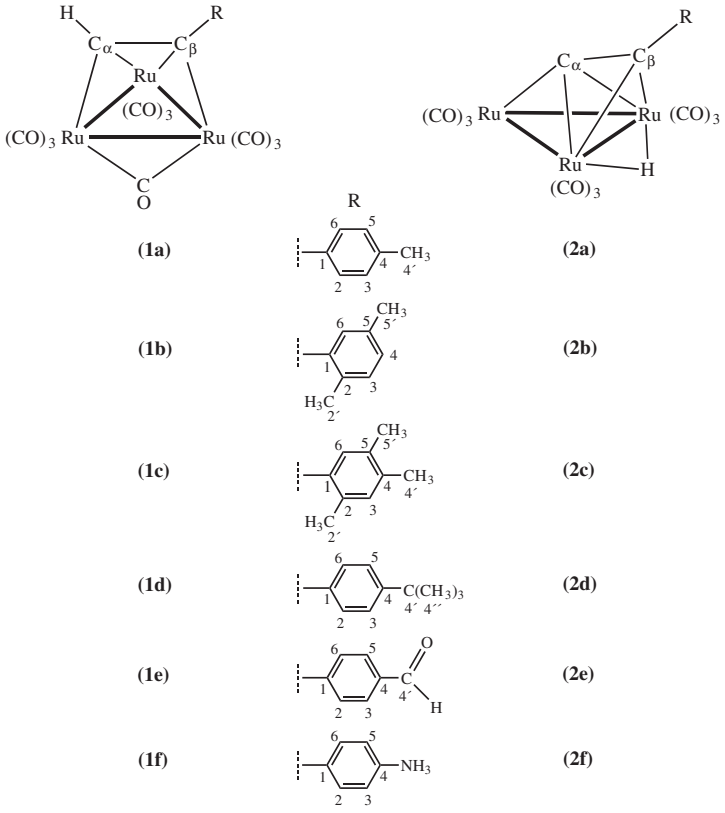

Scheme 1. Structures of acetylene and acetylide ruthenium cluster series **1** and **2**.

Table 1
^{1}H and ^{13}C{^{1}H} NMR data for compound series **1** and **2**.

	^{1}H δ(ppm) J(Hz)	^{13}C{^{1}H} δ(ppm) J(Hz)	$[C_\alpha + C_\beta]$ $\{C_\alpha - C_\beta\}$		^{1}H δ(ppm) J(Hz)	^{13}C{^{1}H} δ(ppm) J(Hz)	$[C_\alpha + C_\beta]$ $\{C_\alpha - C_\beta\}$
1a	8.75 (s, 1H, H_α) 7.58 ($H_{AA'}$, 2H, H(3,5)) 7.32 ($H_{BB'}$, 2H, H(2,6)) J_{AB}, $J_{A'B'}$ = 8.1, $J_{AA'}$ = 6.4, $J_{BB'}$ = 2.0 2.54 (s, 3H, CH_3(4′))	178.7 (s, 1C, C_β) 145.6 (s, 1C, C(1)) 138.7 (s, 1C, C(4)) 134.6 (s, 1C, C_α) 129.2 (s, 2C, C(3,5) 126.0 (s, 2C, C(2,6) 21.3 (s, 1C, C4′)	[313.3] {−44.1}	2a	7.46 ($H_{AA'}$, 2H, H(2,6)) 7.17 ($H_{BB'}$, 2H, H(3,5)) J_{AB}, $J_{A'B'}$ = 8.1, $J_{AA'}$ = 6.4, $J_{BB'}$ = 2.0 2.38 (s, 3H, CH_3(4′)) −20.52 (s, 1H, M–H–M)	166.8 (s, 1C, C_α) 139.0 (s, 1C, C(4)) 131.2 (s, 2C, C(2,6)) 131.0 (s, 1C, C(1)) 129.9 (s, 2C, C(3,5)) 91.4 (s, 1C, C_β) 21.5 (s, 1C, C(4′))	[258.2] {75.4}
1b	8.36 (m, 1H, H_α) 7.07 (d, 1H, H(4)) $^3J^1_{H-}{}^1_H$ = 8.0 6.89 (d, 1H, H(3)) $^3J^1_{H-}{}^1_H$ = 8.0 6.82 (s, 1H, H(6)) 2.37 (s, 3H, CH_3(2′)) 2.27 (s, 3H, CH_3(5′))	176.7 (s, 1C, C_β) 146.7 (s, 1C, C_α) 135.5 (s, 1C, C(1)) 133.0 (s, 1C, C(5)) 130.7 (s, 1C, C(3)) 129.0 (s, 1C, C(2)) 127.7 (s, 1C, C(6)) 127.6 (s, 1C, C(4)) 21.8 (s, 1C, C(2′)) 21.1 (s, 1C, C(5′))	[323.4] {−30.0}	2b	7.24 (s, 1H, H(6)) 7.15 (d, 1H, H(3)) $^3J^1_{H-}{}^1_H$ = 8.0 7.03 (d, 1H, H(4)) $^3J^1_{H-}{}^1_H$ = 8.0 2.51 (s, 3H, CH_3(2′)) 2.33 (s, 3H, CH_3(5′)) −20.40 (s, 1H, M–H–M)	167.5 (s, 1C, C_α) 136.2 (s, 1C, C(5)) 135.7 (s, 1C, C(1)) 133.2 (s, 1C, C(2)) 132.5 (s, 1C, C(6)) 130.0 (s, 1C, C(3)) 129.5 (s, 1C, C(4)) 88.2 (s, 1C, C_β) 22.5 (s, 1C, C(2′)) 21.0 (s, 1C, C(5′))	[255.7] {79.3}
1c	8.44 (s, 1H, H_α) 7.28 (s, 1H, H(3)) 7.01 (s, 1H, H(6)) 2.42 (s, 3H, CH_3(2′)) 2.26 (s, 3H, CH_3(5′)) 2.23 (s, 3H, CH_3(4′))	178.0 (s, 1C, C_β) 145.7 (s, 1C, C_α) 138.1 (s, 1C, C(1)) 137.7 (s, 1C, C(4)) 134.9 (s, 1C, C(5)) 133.8(s, 1C, C(2)) 133.5 (s, 1C, C(3)) 131.0 (s, 1C, C(6)) 20.0 (s, 1C, C(2′)) 19.8 (s, 1C, C(5′)) 19.1 (s, 1C, C(4′))	[323.7] {−32.3}	2c	7.20 (s, 1H, H(6)) 7.05 (s, 1H, H(3)) 2.49 (s, 3H, CH_3(2′)) 2.27 (s, 3H, CH_3(5′)) 2.24 (s, 3H, CH_3(4′)) −20.36 (s, 1H, M–H–M)	167.0 (s, 1C, C_α) 137.6 (s, 1C, C(5)) 136.2 (s, 1C, C(2)) 134.9 (s, 1C, C(4)) 133.0 (s, 1C, C(6)) 131.4 (s, 1C, C(3)) 131.0 (s, 1C, C(1)) 88.4 (s, 1C, C_β) 22.2 (s, 1C, C(2′)) 19.6 (s, 1C, C(5′)) 19.4 (s, 1C, C(4′))	[255.4] {78.6}
1d	8.57 (s, 1H, H_α) 7.29 ($H_{BB'}$, 2H, H(3,5)) 7.13 ($H_{AA'}$, 2H, H(2,6)) J_{AB}, $J_{A'B'}$ = 8.1, $J_{AA'}$ = 6.4, $J_{BB'}$ = 2.0 1.30 (s, 9H, H(4″))	175.3 (s, 1C, C_β) 149.3 (s, 1C, C(4)) 143.2 (s, 1C, C(1)) 133.0 (s, 1C, C_α) 124.1 (s, 2C, C(3,5)) 124.0 (s, 2C, (C2,6)) 36.1 (s, 1C, C(4′)) 32.7 (s, 3C, C(4″))	[308.3] {−42.3}	2d	7.50 ($H_{AA'}$, 2H, H(2,6)) 7.38 ($H_{BB'}$, 2H, H(3,5)) J_{AB}, $J_{A'B'}$ = 8.1, $J_{AA'}$ = 6.4, $J_{BB'}$ = 2.0 1.35 (s, 9H, H(4″) −20.49 (s, 1H, M–H–M)	164.0 (s, 1C, C_α) 149.8 (s, 1C, C(4)) 129.3 (s, 2C, C(2,6)) 129.2 (s, 1C, C(1)) 124.6 (s, 2C, C(3,5)) 90.9 (s, 1C, C_β) 36.3 (s, 1C, C(4′)) 32.8 (s, 3C, C(4″))	[254.9] {73.1}
1e	9.96 (s, 1H, COH) 8.73 (s, 1H, H_α) 7.78 ($H_{AA'}$, 2H, H(3,5)) 7.27 ($H_{BB'}$, 2H, H(2,6)) J_{AB}, $J_{A'B'}$ = 8.1, $J_{AA'}$ = 6.4, $J_{BB'}$ = 2.0	191.5 (s, 1C, COH) 173.7 (s, 1C, C_β) 154.8 (s, 1C, C(4) 140.3 (s, 1C, C_α) 135.9 (s, 1C, C(1) 130.3 (s, 2C, C(3,5)) 126.9 (s, 2C, C(2,6))	[314.0] {−33.4}	2e	10.02 (s, 1H, COH) 7.88 ($H_{AA'}$, 2H, H(3,5)) 7.69 ($H_{BB'}$, 2H, H(2,6)) J_{AB}, $J_{A'B'}$ = 8.1, $J_{AA'}$ = 6.4, $J_{BB'}$ = 2.0 –20.61 (s, 1H, M–H–M)	191.2 (s, 1C, COH) 165.5 (s, 1C, C_α) 141.9 (s, 1C, C(4)) 135.9 (s, 1C, C(1)) 131.6 (s, 2C, C(3,5)) 130.5 (s, 2C, C(2,6)) 88.9 (s, 1C, C_β)	[254.4] {76.6}
1f	8.41 (s, 1H, H_α) 7.04 ($H_{AA'}$, 2H, H(2,6)) 6.54 ($H_{BB'}$, 2H, H(3,5)) J_{AB}, $J_{A'B'}$ = 8.1, $J_{AA'}$ = 6.4, $J_{BB'}$ = 2.0 3.78 (br, 2H, NH_2)	181.9 (s, 1C, C_β) 147.2 (s, 1C, C_α) 144.8 (s, 1C, C4) 128.1 (s, 2C, C(2,6) 125.4 (s, 1C, C1) 120.1 (s, 2C, C(3,5))	[329.1] {−34.7}	2f	7.37 ($H_{AA'}$, 2H, H(3,5)) 6.63 ($H_{BB'}$, 2H, H(2,6)) J_{AB}, $J_{A'B'}$ = 8.1, $J_{AA'}$ = 6.4, $J_{BB'}$ = 2.0 3.88 (a, 2H, NH_2) −20.42 (s, 1H, M–H–M)	165.0 (s, 1C, C_α) 147.1 (s, 1C, C(4)) 132.7 (s, 2C, C(3,5)) 122.4 (s, 1C, C(1)) 115.1 (s, 2C, C(2,6)) 92.5 (s, 1C, C_β)	[257.5] {72.5}

In $CDCl_3$. s = singlet, d = doublet, br = broad.

reduces this alteration. On the other hand, the $\delta(C_\alpha) - \delta(C_\beta)$ data in the free ligands range from 1.5 to 9.4 ppm; the largest polarization upon coordination was found in the acetylide derivatives due to the C–H bond breaking, as observed from the $\delta(C_\alpha) - \delta(C_\beta)$ data (72.5–79.3 ppm for the acetylide compounds; 30.0–44.1 ppm for the parallel alkynyl derivatives). The analysis of the overall data did not show a clear tendency; neither charge alteration nor bond polarization could be correlated with the electronic properties of the substituents in the phenyl rings. Nevertheless, we observed that the presence of the aromatic systems reduces the charge alteration and increases the bond polarization in the perpendicular derivatives when our compounds were compared with the compound [$Ru_3(CO)_9(\mu$-H){μ_3-η^2-(⊥)-C≡C^{t}Bu}], where there is an electron donating group directly attached to the triple bond, [($\delta(C_\alpha) + \delta(C_\beta)$ = 278.2 and $\delta(C_\alpha) - \delta(C_\beta)$ = 56.4 ppm] [18].

The chemical shifts of the *ipso* C1 atom of the substituted aromatic rings in the parallel acetylene clusters **1** were found at higher frequencies (135.5–149.4 ppm) in comparison with the same carbon atom in the acetylide derivatives (122.4–35.9 ppm). A similar behavior has been observed in the CH group of the acetylene ligand when compared to the free ligand; these trends could be due to a diamagnetic deshielding effect produced by the metallic cluster.

In order to stabilize the alkynyl parallel coordination μ_3-η^2-(//) binding mode in these complexes, by taking advantage of a bulky μ-ligand previously attached to the metallic cluster, the reactions of [$Ru_3(CO)_{10}(\mu$-diphosphine)] clusters [diphosphine: dppe = 1, 2-bis(diphenylphosphino)ethane or dfppe = 1,2-bis(dipentafluoro phenylphosphino)ethane] with methyl-substituted aryl alkynes (ligands **a** to **c**, Scheme 2) were studied. Thus, we firstly carried out the reaction of [$Ru_3(CO)_{10}(\mu$-dppe)] with one equivalent of a terminal alkyne HC≡CR [R = C_6H_4-4-CH_3 (**a**), C_6H_3-2,5-$(CH_3)_2$ (**b**), C_6H_2-2,4,5-$(CH_3)_3$ (**c**)] in hot toluene for 1 h. The reaction yielded, however, exclusively the μ_3-η^2-(⊥) acetylide cluster of general formula [$Ru_3(CO)_7(\mu$-dppe)(μ-H){μ_3-η^2-(⊥)-C≡CR}] in moderate yields (**3a**, 62%; **3b**, 59%; **3c**, 65%). Some other milder reaction conditions were also tested; nevertheless, the starting diphosphine cluster remained unchanged. We also studied the reaction of [$Ru_3(CO)_{10}(\mu$-dfppe)], a more Lewis acidic cluster, with one

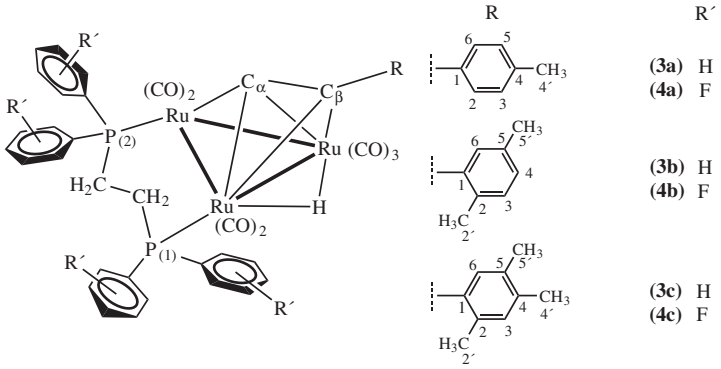

Scheme 2. Structures of acetylide-diphosphine ruthenium cluster series **3** and **4**.

equivalent of a terminal alkyne **a–c**, in THF at 60 °C for 1 h, resulting, once again, in the formation of the analogous acetylide compounds observed for the **3a–c** series $[Ru_3(CO)_7(\mu\text{-dfppe})(\mu\text{-H})\{\mu_3\text{-}\eta^2\text{-}(\perp)\text{-C}{\equiv}\text{CR}\}]$ (**4a**, 60%; **4b**, 65%; **4c**, 63%), Scheme 2. Milder reaction conditions were needed in order to obtain these clusters due to the electronic properties of the perfluorated diphosphine. Under the reaction conditions explored, we were unable to obtain the clusters bearing the parallel coordination mode of the alkyne. An inverse method of synthesis of compounds **3a–c** and **4a–c** was attempted, i.e. the addition of the corresponding diphosphine to the acetylide complexes **2a–c** in a 1:1 stoichiometric ratio; however, no reaction was observed, in spite of the different reaction conditions used such as $MeCN/CH_2Cl_2$ with Me_3NO as activating agent at room temperature, $[Ph_2CO]^-$ catalyst in THF at room temperature or refluxing hexane.

Table 2 shows the ^1H and $^{13}C\{^1H\}$ NMR spectroscopic data of the diphosphine compounds **3a–c** and **4a–c**. The hydride signals for the dppe series were observed, in average, at higher frequencies (−19.60 ppm) than the dfppe series (−20.26 ppm) or CO **2a–c** series (−20.43 ppm), which agrees with the presence of a better σ-donor ligand. The analysis and comparison of the $\delta(C_\alpha) + \delta(C_\beta)$ data in these series showed that the charge alteration increases from compounds **2a–c** to **3a–c** to **4a–c**, $[\delta(C_\alpha) + \delta(C_\beta)$: 254.4–258.2 ppm at CO series, 261.6–263.7 ppm at dppe series, and 264.8–266.6 ppm at dfppe series]. This charge alteration is related to the presence of different ligands attached to the clusters where the electron donating properties of these ligands alter the charge on the metal in the order CO < dppe < dfppe. On the other hand, the $\delta(C_\alpha) - \delta(C_\beta)$ data showed that the largest polarization of the C≡C bonds is present when the perfluorated diphosphine is coordinated to the cluster, showing a dfppe > dppe ≅ CO tendency, $[\delta(C_\alpha) - \delta(C_\beta)$: 72.5–79.3 ppm for the CO series, 75.5–78.2 ppm for the dppe series, and 79.4–81.7 ppm for dfppe series)], this trend can be related to the electron withdrawing properties of the fluorinated rings in the diphosphine. The *ipso* C1 carbon atoms in the diphosphine acetylide derivatives were found at similar frequencies (132.3–136.0 ppm) than their analogous CO acetylides, **1a–c**.

The $^{31}P\{^1H\}$ and $^{19}F\{^1H\}$ NMR data are showed in Table 3. It was observed for compounds **3a–c**, (dppe series) that the chemical shift of the phosphorus atom $P_{(2)}$ attached to the ruthenium atom bonded to the C_α of the acetylide through the σ-bond, is shifted to higher frequencies, due to an increase in electron density on this metal atom. The tendency is reversed when the fluorinated diphosphine was used in clusters **4a–c**; the signal for $P_{(2)}$ is observed at lower frequencies than the phosphorus atom $P_{(1)}$; this may be related to the presence of a more Lewis acidic diphosphine. The $^{19}F\{^1H\}$ spectra of compounds **4a–c** showed signals in the characteristic *ortho*, *para* and *meta* regions, for the four non-equivalent phenyl rings [20].

2.1. X-ray diffraction studies

Single crystal X-ray diffraction studies were carried out; they allowed us to confirm the solid state structures of the **2b–d** and **3b** compounds. ORTEP diagrams of the structures are shown in Figs. 1–4 and Table 4 collects some selected bond lengths and angles. Compound **2c** contains two crystallographically independent molecules in the asymmetric unit; both are essentially identical and only one of the two molecules is showed in Fig. 2; the compound **2d** displays a positional disorder. The structures of these compounds showed the perpendicular coordination of the acetylide group. In compounds **2b–2d** the Ru(1)–Ru(2) distances range from 2.7973(3) to 2.8074(11) Å while the dppe derivative **3b** has the longest bond distance 2.8086(7) Å. This Ru(1)–Ru(2) bond is μ-bridged by a coordinated hydride ligand, confirmed by ^1H NMR data in solution (see above). Similar distances have been reported for the structures of the analogous compounds: **2a** (2.7925(9) Å) [16], $[Ru_3(CO)_9(\mu\text{-H})\{\mu_3\text{-}\eta^2\text{-}(\perp)\text{-C}{\equiv}\text{CR}\}]$ [R = $SiMe_3$ (2.7955 Å); $SiPh_3$ 2.7960 Å) [18], and the longest one for compound **2f** (2.8113 Å) [17]. The other two bond distances Ru(2)–Ru(3) and Ru(3)–Ru(1) are significantly different; the longest distances range from 2.8121(6) to 2.8484(6) Å and the shorter from 2.7827(11) to 2.7973(6) Å. The largest difference between the shortest and the longest bonds is observed in **3b** (0.06 Å). These bond distances are shorter than the[2] reported Ru–Ru bond distance in $[Ru_3(CO)_{12}]$ (2.854 Å av.) [21].

All the C(1)–C(2) distances ranging from 1.292(8) to 1.314(8) Å in the acetylide fragments are close to the normal C–C double bond distance (C_{sp2}–C_{sp2} 1.34 Å [22]) reflecting the change in hybridization of these carbons upon coordination. The C=C bond distance reported for compound **2f** is 1.314(6) Å; thus we observe that the bond distance increases in the order **2b** < **2c** < **2d** < **2f** ≅ **3b**, which can be related to the polarization in the C–C bond of the coordinated acetylide.

The Ru(3)–C(1)–C(2) angles of the acetylide clusters are in the 152.9(4)–156.4(2)° range, while the C(1)–C(2)–C(3) angles are somewhat smaller [143.6(5)–145.2(6)°]. The C(1)–C(2)–C(3) angles increase according to **3b** (143.6(5)°) < **2c** (144.4° av) ≅ **2d** (144.3° av) < **2b** (145.2(6)°) ≅ **2f** (145.5(4)° [17]; this trend can be associated with a decrease in the number of substituents in the phenyl rings, as well as with the type of the substituent. In the case of **3b**, the coordination of the dppe ligand, with a larger steric hindrance than the carbonyl substituents, causes a smaller angle.

The angles formed by the C(1)–C(2) vector and the plane formed by the three metal atoms in the acetylide compounds have different values [17.36(3)–20.21(2)°] depending on the phenyl ring substituents; the order observed was **3b** < **2b** < **2d** < **2c** (19.83° av), and this situation is probably also associated with the inherent hindrance properties of the ligands. On the other hand, the type

Table 2
^{1}H and $^{13}C\{^{1}H\}$ NMR data for compound series **3** and **4**.

	^{1}H δ(ppm) J(Hz)	$^{13}C\{^{1}H\}$ δ(ppm) J(Hz)	$[C_\alpha + C_\beta]$ $\{C_\alpha - C_\beta\}$		^{1}H δ(ppm) J(Hz)	$^{13}C\{^{1}H\}$ δ(ppm) J(Hz)	$[C_\alpha + C_\beta]$ $\{C_\alpha - C_\beta\}$
3a	7.99 (m, 1H, H_p) 7.79 (m, 1H, H_p) 7.51 (m, 4H, $H_{o,m}$) 7.47 (m, 4H, $H_{o,m}$) 7.07 ($H_{AA'}$, 2H, H(2,6)) 6.86 (m, 1H, H_p) 6.76 ($H_{BB'}$, 2H, H(3,5)) J_{AB}, $J_{A'B'}$ = 8.1, $J_{AA'}$ = 6.4, $J_{BB'}$ = 1.9 6.68 (m, 1H, H_p) 2.29 (m, 2H, CH_2) 2.27 (s, 3H, CH_3(4·)) 1.75 (m, 2H, CH_2) −19.62 (AXY, 1H, M–H–M) $^{2}J^{1}_{H-}{}^{31}_{P(1)}$ = 31.3 $^{3}J^{1}_{H-}{}^{31}_{P(2)}$ = 1.8	207.7 (d, 1C, CO) $^{2}J^{1}_{H-}{}^{31}_{P}$ = 12.5 203.8 (d, 1C, CO) $^{2}J^{1}_{H-}{}^{31}_{P}$ = 8.6 201.4 (s,br, 1C, CO) 200.5 (br, 1C, CO) 197.8 (d, 1C, CO) $^{2}J^{1}_{H-}{}^{31}_{P}$ = 13.3 192.0 (br, 1C, CO) 190.1 (br, 1C, CO) 169.6 (s, 1C, C_α) 139.3 (d, 1C, C_i) $^{1}J^{1}_{H-}{}^{31}_{P}$ = 47.4 136.9 (d, 1C, C_i) $^{1}J^{1}_{H-}{}^{31}_{P}$ = 46.3 136.0 (s, 1C, C(4)) 135.1 (d, 2C, C_o) $^{2}J^{1}_{H-}{}^{31}_{P}$ = 13.1 134.5 (d, 1C, C_i) $^{1}J^{1}_{H-}{}^{31}_{P}$ = 43.7 134.5 (s, 1C, C(1)) 133.7 (d, 2C, C_o) $^{2}J^{1}_{H-}{}^{31}_{P}$ = 10.1 132.7(d, 1C, C_i) $^{1}J^{1}_{H-}{}^{31}_{P}$ = 49.5 131.3 (d, 2C, C_p) $^{4}J^{1}_{H-}{}^{31}_{P}$ = 3.4 131.0 (s, 2C, C(2,6)) 130.0 (d, 2C, C_m) $^{3}J^{1}_{H-}{}^{31}_{P}$ = 9.3 129.8 (d, 2C, C_p) $^{4}J^{1}_{H-}{}^{31}_{P}$ = 3.3 129.5 (d, 2C, C_m) $^{3}J^{1}_{H-}{}^{31}_{P}$ = 8.7 129.3 (s, 2C, C(3,5)) 129.1 (d, 2C, C_o) $^{2}J^{1}_{H-}{}^{31}_{P}$ = 11.4 128.9 (d, C, C_m) $^{3}J^{1}_{H-}{}^{31}_{P}$ = 10.8 128.7 (d, 2C, C_o) $^{2}J^{1}_{H-}{}^{31}_{P}$ = 13.8 127.9 (d, 2C, C_m) $^{3}J^{1}_{H-}{}^{31}_{P}$ = 9.3 94.1 (s, 1C, C_β) 26.0 (d, 1C, CH_2) $^{1}J^{1}_{H-}{}^{31}_{P}$ = 28.8 21.5 (d, 1C, CH_2) $^{1}J^{1}_{H-}{}^{31}_{P}$ = 22.2 21.3 (s, 1C, C(4·))	[263.7] {75.5}	**4a**	7.13 ($H_{AA'}$, 2H, H(2,6)) 6.92 ($H_{BB'}$, 2H, H(3,5)) J_{AB}, $J_{A'B'}$ = 8.1, $J_{AA'}$ = 6.4, $J_{BB'}$ = 1.9 2.92 (m, 2H, CH_2) 2.25 (s, 3H, CH_3 4·) 1.87 (m, 2H, CH_2) −20.34 (AXY, 1H, M–H–M) $^{2}J^{1}_{H-}{}^{31}_{P(1)}$ = 46.9 $^{3}J^{1}_{H-}{}^{31}_{P(2)}$ = 1.8	205.7 (br, 1C, CO) 202.5 (br, 1C, CO) 198.7 (br, 1C, CO) 198.2 (br, 1C, CO) 194.6 (br, 1C, CO) 189.6 (br, 1C, CO) 187.7 (br, 1C, CO) 173.0 (s, 1C, C_α) 149.6 (m, 4C, C_o) 147.1 (m, 4C, C_o) 145.8 (m, 2C, C_p) 143.8 (m, 2C, C_p) 142.6 (m, 2C, C_i) 139.4 (m, 4C, C_m) 138.6 (m, 2C, C_i) 138.0 (s, 1C, C(4)) 136.8 (m, 4C, C_m) 132.6 (s, 1C, C(1)) 130.9 (s, 2C, C(2,6)) 129.4 (s, 2C, C(3,5)) 93.6 (s, 1C, C_β) 27.1 (d, 1C, CH_2) $^{1}J^{13}_{C-}{}^{31}_{P}$ = 27.0 24.0 (d, 1C, CH_2) $^{1}J^{13}_{C-}{}^{31}_{P}$ = 25.3 21.2 (s, 1C, C(4·))	[266.6] {79.4}
3b	7.99 (m, 1H, H_p) 7.80 (m, 1H, H_p) 7.52 (m, 8H, $H_{o,m}$) 7.46 (m, 8H, $H_{o,m}$) 6.92 (d, 1H, H(4)) 6.78 (m, 1H, H_p) 6.69 (m, 1H, H_p) 6.61 (d, 1H, H(3)) $^{3}J_{1H\text{-}1H}$ = 8.0 6.48 (s, 1H, H(6)) 2.73 (s, 3H, CH_3(5·)) 2.38 (m, 2H, CH_2) 1.94 (s, 3H, CH_3(2·)) 1.78 (m, 2H, CH_2) −19.56 (AXY, 1H, M–H–M) $^{2}J^{1}_{H-}{}^{31}_{P(1)}$ = 30.6 $^{3}J^{1}_{H-}{}^{31}_{P(2)}$ = 1.6	208.1 (d, 1C, CO) $^{2}J^{1}_{H-}{}^{31}_{P}$ = 10.3 203.9 (d, 1C, CO) $^{2}J^{1}_{H-}{}^{31}_{P}$ = 8.7 201.3 (br, 1C, CO) 200.5 (d, 1C, CO) $^{2}J^{1}_{H-}{}^{31}_{P}$ = 9.9 198.1 (d, 1C, CO) $^{2}J^{1}_{H-}{}^{31}_{P}$ = 11.7 192.3 (br, 1C, CO) 189.7 (br, 1C, CO) 170.0 (s, 1C, C_α) 139.3 (d, 1C, C_i) $^{1}J^{1}_{H-}{}^{31}_{P}$ = 47.2 136.8 (d, 1C, C_i) $^{1}J^{1}_{H-}{}^{31}_{P}$ = 47.6 136.0 (s, 1C, C(1)) 135.2 (s, 1C, C(2)) 135.1 (d, 2C, C_o) $^{2}J^{1}_{H-}{}^{31}_{P}$ = 13.1 134.5(d, 1C, C_i) $^{1}J^{1}_{H-}{}^{31}_{P}$ = 42.3 134.5 (s, 1C, C(5)) 133.9 (d, 2C, C_o) $^{2}J^{1}_{H-}{}^{31}_{P}$ = 11.1	[261.8] {78.2}	**4b**	7.09 (d, 1H, H(4)) 6.89 (d, 1H, H(3)) $^{3}J^{1}_{H-}{}^{1}_{H}$ = 7.8 6.73 (s, 1H, H(6)) 2.98 (m, 2H, CH_2) 2.58 (s, 3H, CH_3(5·)) 2.14 (s, 3H, CH_3(2·)) 1.99(m, 2H, CH_2) −20.24 (AXY, 1H, M–H–M) $^{2}J^{1}_{H-}{}^{31}_{P(1)}$ = 46.5 $^{3}J^{1}_{H-}{}^{31}_{P(2)}$ = 2.1	204.5 (br, 1C, CO) 202.7 (br, 1C, CO) 198.6 (br, 1C, CO) 198.2 (br, 1C, CO) 194.9 (br, 1C, CO) 189.7 (br, 1C, CO) 187.3 (br, 1C, CO) 173.3 (s, 1C, C_α) 149.6 (m, 4C, C_o) 147.1 (m, 4C, C_o) 146.1 (m, 2C, C_p) 143.8 (m, 2C, C_p) 141.4 (m, 2C, C_i) 139.4 (m, 4C, C_m) 138.8 (m, 2C, C_i) 136.9 (m, 4C, C_m) 136.6 (s, 1C, C(5)) 135.8 (s, 1C, C(1)) 134.6 (s, 1C, C(2)) 131.2 (s, 1C, C(6)) 130.0 (s, 1C, C(3)) 128.0 (s, 1C, C(4)) 91.7 (s, 1C, C_β) 27.2 (d, 1C, CH_2) $^{1}J^{13}_{C-}{}^{31}_{P}$ = 29.7	[264.8] {81.4}

Table 2 (*continued*)

	^{1}H δ(ppm) J(Hz)	^{13}C{^{1}H} δ(ppm) J(Hz)	$[C_\alpha + C_\beta]$ $\{C_\alpha - C_\beta\}$		^{1}H δ(ppm) J(Hz)	^{13}C{^{1}H} δ(ppm) J(Hz)	$[C_\alpha + C_\beta]$ $\{C_\alpha - C_\beta\}$
		132.5(d, 1C, C_i) $^1J^1_{H-}{}^{31}{}_P$ = 48.0 132.3 (s, 1C, C(6)) 131.4 (s, 1C, C_p) 131.2 (d, 1C, C_p) $^4J^1_{H-}{}^{31}{}_P$ = 1.8 130.0 (d, 2C, C_m) $^3J^1_{H-}{}^{31}{}_P$ = 10.0 129.8 (d, 1C, C_p) $^4J^1_{H-}{}^{31}{}_P$ = 2.3 129.1 (d, 2C, C_m) $^3J^1_{H-}{}^{31}{}_P$ = 9.9 129.1(s, 1C, C_p) 129.0 (s, 1C, C(4)) 128.8 (d, 2C, C_o) $^2J^1_{H-}{}^{31}{}_P$ = 12.8 128.7 (d, 2C, C_o) $^3J^1_{H-}{}^{31}{}_P$ = 12.1 128.5 (d, 2C, C_m) $^2J^1_{H-}{}^{31}{}_P$ = 10.5 127.6(d, 2C, C_m) $^3J^1_{H-}{}^{31}{}_P$ = 9.9 127.1 (s, 1C, C(3)) 91.8 (s, 1C, C_β) 25.7 (d, 1C, CH_2) $^1J^1_{H-}{}^{31}{}_P$ = 26.9 21.4 (d, 1C, CH_2) $^1J^1_{H-}{}^{31}{}_P$ = 25.0 20.8 (s, 1C, C(5′)) 14.2 (s, 1C, C(2′))				24.4 (d, 1C, CH_2) $^1J^{13}_{C-}{}^{31}{}_P$ = 23.3 21.4 (s, 1C, C(5′)) 20.5 (s, 1C, C(2′))	
3c	7.91 (m, 1H, H_p) 7.71 (m, 1H, H_p) 7.44 (m, 8H, $H_{o,m}$) 7.36 (m, 8H, $H_{o,m}$) 6.73 (s, 1H, H(3)) 6.59 (m, 1H, H_p) 6.48 (m, 1H, H_p) 6.36 (s, 1H, H(6)) 2.62 (s, 3H, CH_3(2′)) 2.30 (m, 2H, CH_2) 2.07 (s, 3H, CH_3(4′)) 1.76 (s, 3H, CH_3(5′)) 1.67 (m, 2H, CH_2) −19.62 (AXY, 1H, M–H–M) $^2J^1_{H-}{}^{31}{}_{P(1)}$ = 30.6 $^3J^1_{H-}{}^{31}{}_{P(2)}$ = 1.8	208.2 (d, 1C, CO) $^2J^1_{H-}{}^{31}{}_P$ = 12.3 203.9 (d, 1C, CO) $^2J^1_{H-}{}^{31}{}_P$ = 7.2 201.4 (s,br, 1C, CO) 200.6 (d, 1C, CO) $^2J^1_{H-}{}^{31}{}_P$ = 8.6 198.1 (d, 1C, CO) $^2J^1_{H-}{}^{31}{}_P$ = 12.3 192.3 (br, 1C, CO) 189.8 (br, 1C, CO) 169.6 (s, 1C, C_α) 139.4 (d, 1C, C_i) $^1J^{13}_{C-}{}^{31}{}_P$ = 48.3 136.9 (d, 1C, C_i) $^1J^{13}_{C-}{}^{31}{}_P$ = 48.9 135.1 (d, 2C, C_o) $^2J^{13}_{C-}{}^{31}{}_P$ = 12.9 134.9 (s, 1C, C(2)) 134.7 (s, 1C, C(4)) 134.2 (d, 1C, C_i) $^1J^{13}_{C-}{}^{31}{}_P$ = 50.7 133.9 (d, 4C, C_o) $^2J^{13}_{C-}{}^{31}{}_P$ = 11.0 133.7 (s, 1C, C(6)) 133.2 (s, 1C, C(1)) 133.1 (s, 1C, C(5)) 132.6 (d, 1C, C_i) $^1J^{13}_{C-}{}^{31}{}_P$ = 48.3 131.4 (d, 1C, C_p) 131.1 (d, 1C, C_p) 130.6 (s, 1C, C(3)) 130.0 (d, 2C, C_m) $^3J^{13}_{C-}{}^{31}{}_P$ = 9.4 129.7 (d, 1C, C_p) 129.1 (d, 2C, C_o) $^3J^{13}_{C-}{}^{31}{}_P$ = 10.1 128.9 (d, 2C, C_o) $^3J^{13}_{C-}{}^{31}{}_P$ = 8.2 128.5 (d, 2C, C_m) $^3J^{13}_{C-}{}^{31}{}_P$ = 9.8 128.2 (s, 1C, C_p) 127.6 (d, 2C, C_m) $^3J^{13}_{C-}{}^{31}{}_P$ = 9.0 92.0 (s, 1C, C_β)	[261.6] {77.6}	**4c**	6.98 (s, 1H, H(3)) 6.67 (s, 1H, H(6)) 2.97 (m, 2H, CH_2) 2.55 (s, 3H, CH_3(2′)) 2.21 (s, 3H, CH_3(4′)) 2.06 (s, 3H, CH_3(5′)) 1.95 (m, 2H, CH_2) −20.21 (AXY, 1H, M–H–M) $^2J^1_{H-}{}^{31}{}_{P(1)}$ = 46.6 $^3J^1_{H-}{}^{31}{}_{P(2)}$ = 2.1	204.6 (br, 1C, CO) 202.8 (br, 1C, CO) 198.7 (br, 1C, CO) 198.1 (br, 1C, CO) 195.1 (br, 1C, CO) 189.9 (br, 1C, CO) 187.4 (br, 1C, CO) 172.9 (s, 1C, C_α) 149.7 (m, 4C, C_o) 147.2 (m, 4C, C_o) 146.1 (m, 2C, C_p) 143.7 (m, 2C, C_p) 141.3 (m, 2C, C_i) 139.4 (m, 4C, C_m) 138.8 (m, 2C, C_i) 137.0 (s, 1C, C(1)) 136.8 (m, 4C, C_m) 136.4 (s, 1C, C(6)) 134.3 (s, 1C, C(3)) 131.9 (s, 1C, C(4)) 131.3 (s, 1C, C(5)) 131.7 (s, 1C, C(2)) 91.9 (s, 1C, C_β) 27.2 (d, 1C, CH_2) $^1J^1_{H-}{}^{31}{}_P$ = 29.6 24.3 (d, 1C, CH_2) $^1J^1_{H-}{}^{31}{}_P$ = 24.6 21.2 (s, 1C, C(2′)) 19.2 (s, 1C, C(4′)) 18.9 (s, 1C, C(5′))	[264.8] {81.7}

(*continued on next page*)

Table 2 (*continued*)

^{1}H δ(ppm) J(Hz)	^{13}C{^{1}H} δ(ppm) J(Hz)	$[C_\alpha + C_\beta]$ $\{C_\alpha - C_\beta\}$	^{1}H δ(ppm) J(Hz)	^{13}C{^{1}H} δ(ppm) J(Hz)	$[C_\alpha + C_\beta]$ $\{C_\alpha - C_\beta\}$
	25.8 (d, 1C, CH_2) $^1J^{13}_{C-}{}^{31}_{P}$ = 25.2 22.5 (s, 1C, C(2′)) 21.5 (d, 1C, CH_2) $^1J^{13}_{C-}{}^{31}_{P}$ = 28.6 19.4 (s, 1C, C(4′)) 19.1 (s, 1C, C(5′))				

In $CDCl_3$, s = singlet, d = doublet, m = multiplet, br = broad. *o*, ortho; *p*, para; *m*, meta; *i*, ipso.

Table 3
^{31}P{^{1}H} and ^{19}F{^{1}H} NMR data for compound series **3** and **4**.

	^{31}P{^{1}H} δ(ppm)		^{31}P{^{1}H} δ(ppm)	^{19}F{^{1}H} δ(ppm) J(Hz)	
3a	57.7 (s) P(2) 44.7 (s) P(1)	**4a**	26.4 (s) P(1) 22.6 (s) P(2)	−126.7 (d, 2F, F_o) −127.5 (d, 2F, F_o) −129.9 (br, 2F, F_o) −132.0 (d, 2F, F_o) $^3J^{19}_{Fo-}{}^{19}_{Fm}$ = 19.2 −143.8 (t, 1F, F_p) −145.1 (t, 1F, F_p)	−148.7 (t, 1F, F_p) −149.5 (t, 1F, F_p) $^3J^{19}_{Fp-}{}^{19}_{Fm}$ = 20.0 −156.4 (br, 2F, F_m) −157.5 (m, 4F, F_m) −158.1 (br, 2F, F_m)
3b	56.3 (s) P(2) 45.7 (s) P(1)	**4b**	26.2 (s) P(1) 22.7 (s) P(2)	−127.3 (d, 2F, F_o) −127.7 (d, 2F, F_o) −130.5 (br, 2F, F_o) −132.0 (d, 2F, F_o) $^3J^{19}_{Fo-}{}^{19}_{Fm}$ = 15.5 −143.9 (t, 1F, F_p)	−145.2 (t, 1F, F_p) −148.8 (t, 1F, F_p) -148.9 (t, 1F, F_p) $^3J^{19}_{Fp-}{}^{19}_{Fm}$ = 20.7 −157.7 (br, 2F, F_m) -158.3 (m, 6F, F_m)
3c	56.3 (s) P(2) 45.8 (s) P(1)	**4c**	26.5 (s) P(1) 22.6 (s) P(2)	−127.2 (d, 2F, F_o) −127.6 (d, 2F, F_o) −130.4 (br, 2F, F_o) −132.0 (d, 2F, F_o) $^3J^{19}_{Fo-}{}^{19}_{Fm}$ = 17.3 −143.8 (t, 1F, F_p) −145.1 (t, 1F, F_p)	−148.8 (t, 1F, F_p) −149.7 (t, 1F, F_p) $^3J^{19}_{Fp-}{}^{19}_{Fm}$ = 23.0 −157.5 (br, 2F, F_m) −158.2 (m, 4F, F_m) −158.6 (br, 2F, F_m)

In $CDCl_3$. s = singlet, d = doublet, m = multiplet, br = broad. *o*, ortho; *p*, para; *m*, meta.

of substituents on C(2) does not affect the perpendicular relation between the C(1)–C(2) and Ru(1)–Ru(2) vectors, with an average of 89.37°; this value is slightly smaller than those reported for the analogous compounds $[Ru_3(CO)_9(\mu\text{-H})\{\mu_3\text{-}\eta^2\text{-}(\perp)\text{-C}{\equiv}\text{CR}\}]$ (R = $SiMe_3$, 89.7°; $SiPh_3$, 89.81°) [18].

For compound **3b**, the P(2) of the diphosphine is roughly located in the plane of the metal atoms [P(2)–Ru_3 triangular plane distance: 0.502 Å], with a dihedral angle P(2)–Ru(2)–Ru(3)–Ru(1) of 167.03(5)°; however the P(1) is located above the metal triangle plane [ca. 1.267 Å] with a dihedral angle P(1)–Ru(1)–Ru(2)–Ru(3) of 146.18(4)°. In **3b** is observed an intramolecular π-stacking interaction between a phenyl ring of the diphosphine dppe and the acetylide ring with a distance of 3.859 Å between centroids. The Ru–P and Ru–C bond lengths agree with the normal values for ruthenium(0).

3. Conclusions

The synthesis of the parallel acetylene and perpendicular acetylide ruthenium trinuclear carbonyl and diphosphine clusters was achieved. In solution, the acetylene **1a**–**f** compounds rapidly convert into the acetylide **2a**–**f** clusters, showing the low stability of the $\mu_3\text{-}\eta^2$ coordination mode based on a π:σ:σ ligand donation.

The analysis of the ^{13}C{^{1}H} chemical shifts of the C_α and C_β atoms in conjunction with the addition and subtraction of the individual chemical shifts, was used to propose the change in polarization or charge on the triple bond due to variations in the aryl substituents, in the modes of coordination, and in the changes of the substituents on the ruthenium cluster.

Under the reaction conditions used, the presence of the diphosphine dppe or dfppe did not produce the desired stabilization of the $\mu_3\text{-}\eta^2$-(//) parallel coordination of the acetylene, showing that the changes in electronic properties of the cluster, at least with this two diphosphines, is not enough to isolate this parallel coordination of the alkyne. The X-ray structures of compounds **2b**–**d** and **3b** showed the thermodynamically stable $\mu_3\text{-}\eta^2$-(⊥) perpendicular mode of the acetylide, without significant changes in structural parameters.

4. Experimental

4.1. General procedures and materials

$[Ru_3(CO)_{10}(NCMe_3)_2]$ [4], $[Ru_3(CO)_{10}(\mu\text{-dppe})]$ [23] and $[Ru_3(CO)_{10}(\mu\text{-dfppe})]$ [20] were prepared by published methods. All chemicals were purchased from Aldrich Company and used as received except for Me_3NO. Trimethylamine *N*-oxide (5 g, 0.065 mmol) was dried using dry DMF (100 mL); the mixture was distilled until reach a volume of 15–20 mL. The resulting needles of the oxide were washed three times with freshly distilled DMF (4 mL) and the residue was filtrated. The white needles were repeatedly sublimed in high vacuum at 100 °C by means of an oil bath until dry bright white needles were obtained. All reactions were performed under a nitrogen atmosphere by using standard Schlenk techniques. Solvents were dried by the standard procedures prior to use. Commercial tlc plates (silica gel 60 F254) were used to monitor the progress of the reactions. Infrared spectra were recorded as a solid thin film on a CsI window on a GX PERKIN Elmer 2000 FT-IR spectrometer or in NaCl cells on a PERKIN Elmer 16FPCF-PIR spectrophotometer. NMR spectra were measured on a JEOL 400 and VARIAN 400 spectrometers in $CDCl_3$, with ^{1}H and ^{13}C spectra relative to $SiMe_4$, ^{31}P spectra relative to 85% aq. H_3PO_4 and ^{19}F

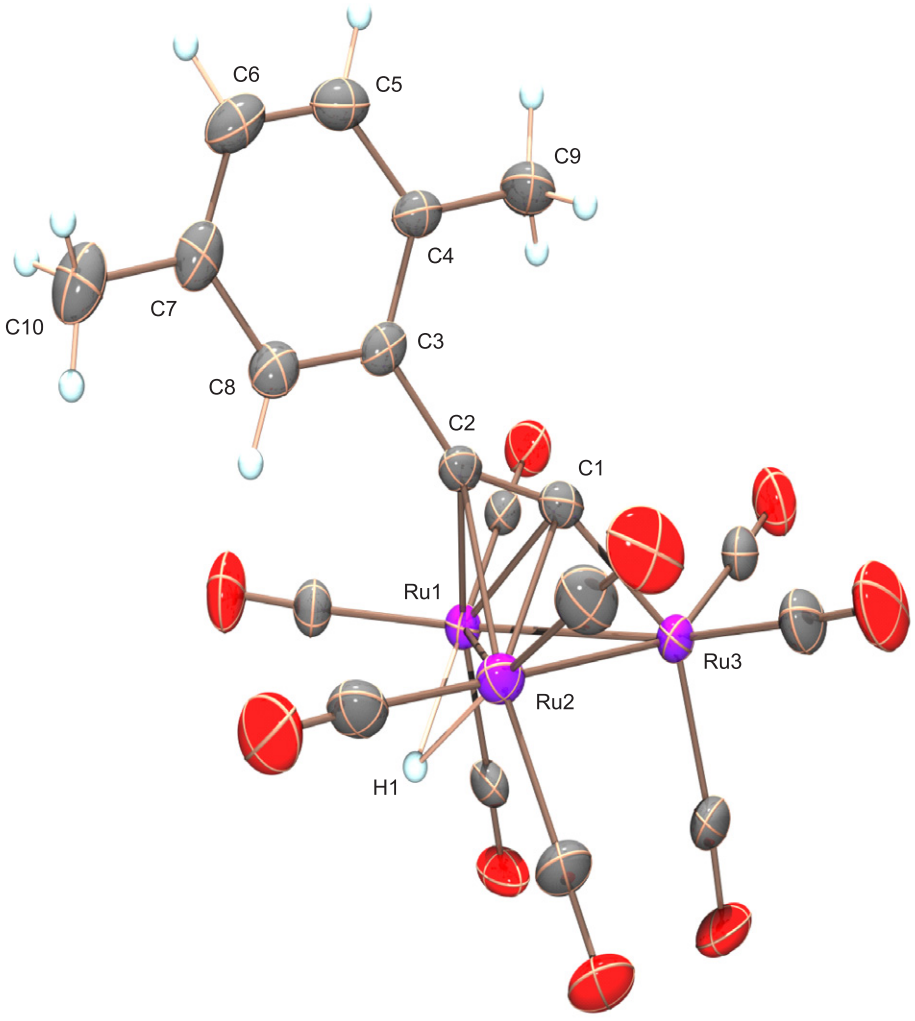

Fig. 1. ORTEP view of compound **2b** (30% probability).

spectra referred to $CFCl_3$. Mass spectrometric measurements performed by direct insertion were recorded on a HR-LC 1100/MSD TOF Agilent Technology equipment at CINVESTAV-México.

4.2. Synthesis of compound $[Ru_3(CO)_{10}(MeCN)_2]$

A solution of dry trimethylamine *N*-oxide, Me_3NO, (13.2 mg, 0.176 mmol) in acetonitrile (4.00 mL) was added dropwise to a solution of $[Ru_3(CO)_{12}]$ (50.0 mg, 0.0780 mmol) in dichloromethane (40.0 mL)/acetonitrile (10.0 mL) at −78 °C, in a dry ice–acetone bath, over a period of 15 min. Then, the solution was removed from the dry ice bath and it was slowly warmed to room temperature, where the complete conversion of $[Ru_3(CO)_{12}]$ into $[Ru_3(CO)_{10}(NCMe)_2]$ (52.0 mg, 0.0780 mmol) had occurred after 15 min approximately (tlc monitored).

4.3. General procedure for the synthesis of compounds 1a–f and 2a–f

An excess of the corresponding alkyne HC≡CR was added to the solution of $[Ru_3(CO)_{10}(NCMe)_2]$ (52.0 mg, 0.0780 mmol) freshly prepared; the solution was stirred at room temperature under N_2 for 30 min displaying a color change, from yellow to red. The solvent was removed under reduced pressure, and the resulting residue was dissolved in a small amount of dichloromethane. The compounds were separated on tlc chromatographic plates [eluent: hexane:$CHCl_3$ (80:20 v/v)]. The yellow first band was identified as the perpendicular derivatives $[Ru_3(CO)_9(\mu\text{-}CO)\{\mu_3\text{-}\eta^2\text{-}(\perp)\text{-}HC{\equiv}CR\}]$ (**2**) and the orange second band corresponded to parallel derivatives $[Ru_3(CO)_9(\mu\text{-}CO)\{\mu_3\text{-}\eta^2\text{-}(//)\text{-}HC{\equiv}CR\}]$ (**1**). *Note: It was not possible to obtain adequate elemental analysis for compounds **1a–f**; due to their inherent instability; they continually are transform to compounds **2a–f**, respectively.*

4.3.1. $[Ru_3(CO)_9(\mu\text{-}CO)\{\mu_3\text{-}\eta^2\text{-}(//)\text{-}HC{\equiv}C\ C_6H_4\text{-}4\text{-}CH_3\}]$ (1a) and $[Ru_3(CO)_9(\mu\text{-}H)\{\mu_3\text{-}\eta^2\text{-}(\perp)\text{-}C{\equiv}C\ C_6H_4\text{-}4\text{-}CH_3\}]$ (2a)

4-Ethynyltoluene (16.0 μL, 0.126 mmol). $[Ru_3(CO)_9(\mu\text{-}CO)\{\mu_3\text{-}\eta^2\text{-}(//)\text{-}HC{\equiv}C\ C_6H_4\text{-}4\text{-}CH_3\}]$ (**1a**); yield: 44.0%, 18.0 mg orange solid. IR ν(CO): 2097(m), 2061(sh), 2055(vs), 2029(w), 2015(sh), 1881(w) cm^{-1}. $[Ru_3(CO)_9(\mu\text{-}H)\{\mu_3\text{-}\eta^2\text{-}(\perp)\text{-}C{\equiv}CC_6H_4\text{-}4\text{-}CH_3\}]$ (**2a**); yield: 21.0%, 8.40 mg, yellow solid. IR ν(CO): 2097(w), 2073(m), 2053(m), 2022(vs), 1986(w) cm^{-1}. HR–MS (ESI–TOF); $[M+H]^-$ for ($C_{18}H_7O_9Ru_3$) Calc. 672.7225, found +672.7220 amu. *Anal.* Calc. for $C_{18}H_8O_9Ru_3$ (671.46): C, 32.20; H, 1.20. Found: C, 32.15; H, 1.18%.

4.3.2. $[Ru_3(CO)_9(\mu\text{-}CO)\{\mu_3\text{-}\eta^2\text{-}(//)\text{-}HC{\equiv}C\ C_6H_3\text{-}2,5\text{-}(CH_3)_2\}]$ (1b) and $[Ru_3(CO)_9(\mu\text{-}H)\{\mu_3\text{-}\eta^2\text{-}(\perp)\text{-}C{\equiv}C\ C_6H_3\text{-}2,5\text{-}(CH_3)_2\}]$ (2b)

1-Ethynyl-2,5-dimethylbenzene (18.0 μL, 0.126 mmol). $[Ru_3(CO)_9(\mu\text{-}CO)\{\mu_3\text{-}\eta^2\text{-}(//)\text{-}HC{\equiv}CC_6H_3\text{-}2,5\text{-}(CH_3)_2\}]$ (**1b**); yield:

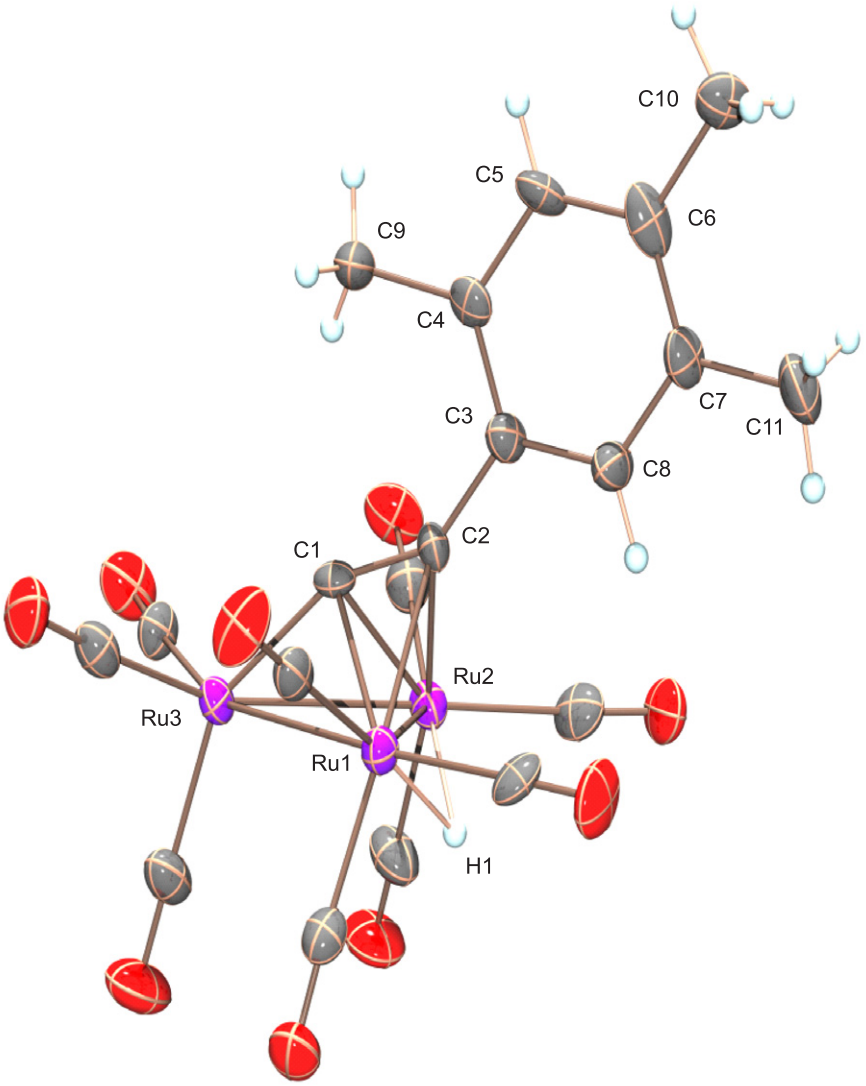

Fig. 2. ORTEP view of compound **2c** (30% probability).

19.0%, 47.0 mg, orange solid. IR ν(CO): 2097(m), 2059(vs), 2029(vs), 2013(sh), 1877(w) cm^{-1}. [$Ru_3(CO)_9(\mu$-H){μ_3-η^2-(⊥)-C≡C C_6H_3-2,5-$(CH_3)_2$}] (**2b**); yield: 23.0%, 9.20 mg, yellow solid. IR ν(CO): 2097(w), 2071(vs), 2053(vs), 2022(vs), 1990(m) cm^{-1}. HR–MS (ESI–TOF); $[M+H]^-$ for ($C_{19}H_9O_9Ru_3$) Calc. 686.7382, found +686.7384 amu. *Anal.* Calc. for $C_{19}H_{10}O_9Ru_3$ (685.49): C, 33.29; H, 1.47. Found: C, 33.54; H, 1.30%.

4.3.3. [$Ru_3(CO)_9(\mu$-CO){μ_3-η^2-(//)-HC≡CC_6H_2-2,4,5-$(CH_3)_3$}] (1c) and [$Ru_3(CO)_9(\mu$-H){μ_3-η^2-(⊥)-C≡CC_6H_2-2,4,5-$(CH_3)_3$}] (2c)

1-Ethynyl-2,4,5-trimethylbenzene (32.0 mg, 0.223 mmol). [$Ru_3(CO)_9(\mu$-CO){μ_3-η^2-(//)-HC≡CC_6H_2-2,4,5-$(CH_3)_3$}] (**1c**); yield: 45.0%, 18.0 mg, orange solid. IR ν(CO): 2096(m), 2049(vs), 2014(vs), 1874(w) cm^{-1}. [$Ru_3(CO)_9(\mu$-H){μ_3-η^2-(⊥)-C≡CC_6H_2-2,4,5-$(CH_3)_3$}] (**2c**); yield: 21.0%, 8.40 mg, yellow solid. IR ν(CO): 2096(m), 2068(vs), 2049(vs), 2013(vs), 1983(s) cm^{-1}. MS (ESI–TOF); $[M-H]^-$ for ($C_{20}H_{11}O_9Ru_3$) Calc. 700.7538, found +700.7549 amu. *Anal.* Calc. for $C_{20}H_{12}O_9Ru_3$ (699.52): C, 34.34; H, 1.73. Found: C, 34.65; H, 1.59%.

4.3.4. [$Ru_3(CO)_9(\mu$-CO){μ_3-η^2-(//)-HC≡CC_6H_4-4-^{t}Bu}] (1d) and [$Ru_3(CO)_9(\mu$-H){μ_3-η^2-(⊥)-C≡CC_6H_4-4-^{t}Bu}] (2d)

1-Ethynyl-4-terbutylbenzene (20.0 μL, 0.111 mmol). [$Ru_3(CO)_9(\mu$-CO){μ_3-η^2-(//)-HC≡CC_6H_4-4-^{t}Bu}] (**1d**); yield: 44.0%, 17.7 mg, orange solid. IR ν(CO): 2097(m), 2050(vs), 2006(vs), 1874(w) cm^{-1}. [$Ru_3(CO)_9(\mu$-H){μ_3-η^2-(⊥)-C≡CC_6H_4-4-^{t}Bu}] (**2d**); yield: 28.0%, 11.2 mg, yellow solid. IR ν(CO): 2098(m), 2051(vs), 2012(vs), 1970(m) cm^{-1}. HR–MS (ESI–TOF); $[M+H]^-$ for ($C_{21}H_{13}O_9Ru_3$) Calc. 714.7695, found +714.7702 amu. *Anal.* Calc. for $C_{21}H_4O_9Ru_3$ (713.53): C, 35.35; H, 1.98. Found: C, 34.79; H, 1.93%.

4.3.5. [$Ru_3(CO)_9(\mu$-CO){μ_3-η^2-(//)-HC≡C C_6H_4-4-COH}] (1e) and [$Ru_3(CO)_9(\mu$-H){μ_3-η^2-(⊥)-C≡C C_6H_4-4-COH}] (2e)

4-Ethynylbenzaldehyde (20.0 mg, 0.153 mmol). [$Ru_3(CO)_9(\mu$-CO){μ_3-η^2-(//)-HC≡CC_6H_4-4-COH}] (**1e**); yield: 43.0%,

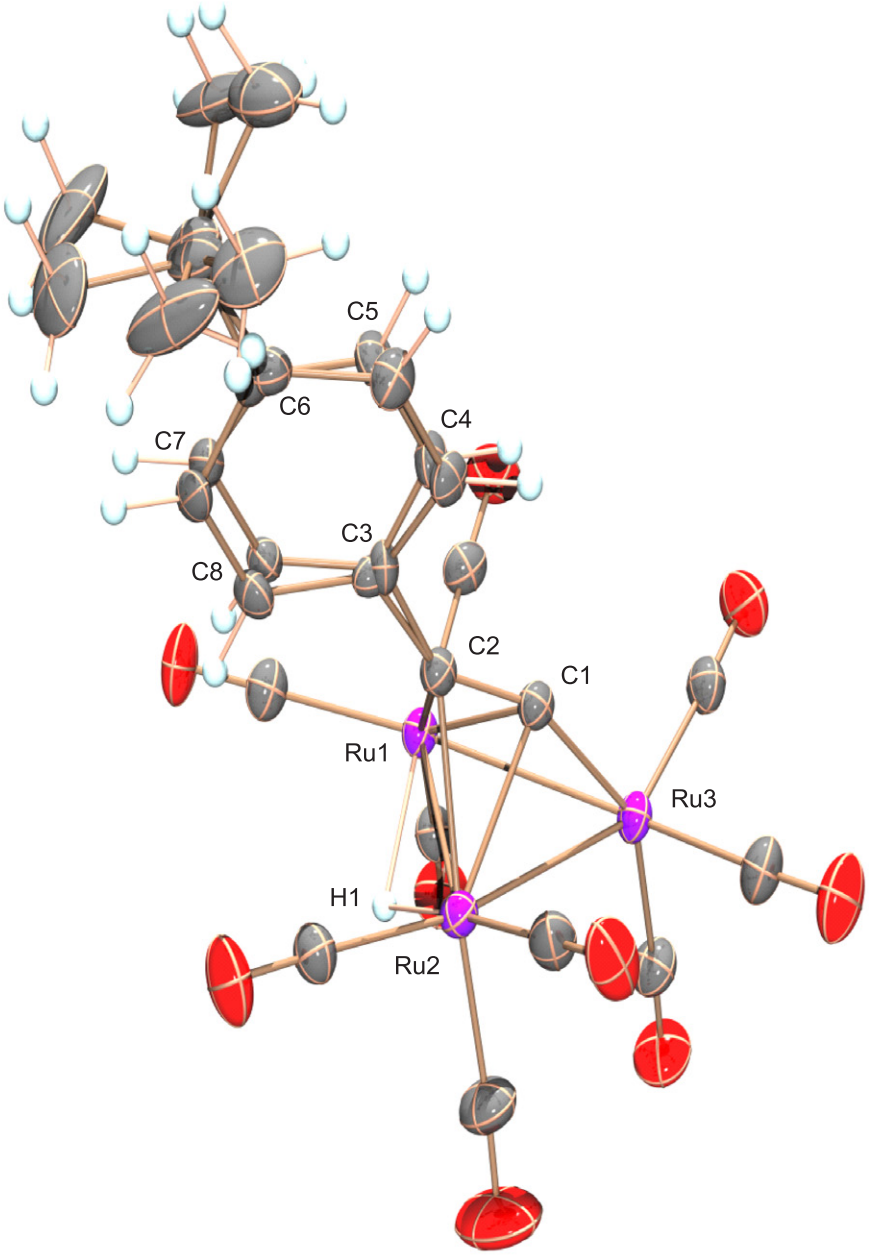

Fig. 3. ORTEP view of compound **2d** (30% probability).

17.3 mg, orange solid. IR ν(CO): 2098(vw), 2076(m), 2066(m), 2056(s), 2036(m), 2026(m), 2016(sh), 1954(w), 1884(vw, br) cm^{-1}. $[Ru_3(CO)_9(\mu\text{-}H)\{\mu_3\text{-}\eta^2\text{-}(\perp)\text{-}C{\equiv}CC_6H_4\text{-}4\text{-}COH\}]$ (**2e**); yield: 17.0%, 6.80 mg, yellow solid. IR ν(CO): 2072(m), 2057(m), 2027(s), 1992(w) cm^{-1}. HR–MS (ESI–TOF); $[M-H]^-$ for ($C_{18}H_5O10Ru_3$) Calc. 686.7018, found +686.7030 amu. *Anal.* Calc. for $C_{18}H_6O_{10}Ru_3$ (685.45): C, 31.54; H, 0.88. Found: C, 32.22; H, 0.86%.

4.3.6. $[Ru_3(CO)_9(\mu\text{-}CO)\{\mu_3\text{-}\eta^2\text{-}(///)\text{-}HC{\equiv}C\ C_6H_4\text{-}4\text{-}NH_2\}]$ (1f) and $[Ru_3(CO)_9(\mu\text{-}H)\{\mu_3\text{-}\eta^2\text{-}(\perp)\text{-}C{\equiv}C\ C_6H_4\text{-}4\text{-}NH_2\}]$ (2f)

4-Ethynyl-aniline (21.0 mg; 0.180 mmol). $[Ru_3(CO)_9(\mu\text{-}CO)\{\mu_3\text{-}\eta^2\text{-}(//)\text{-}HC{\equiv}C\ C_6H_4\text{-}4\text{-}NH_2\}]$ (**1f**); yield: 28.0%, 11.3 mg, orange solid. IR ν(CO): 2095(m), 2046(vs), 2004(vs), 1830(w) cm^{-1}. $[Ru_3(CO)_9(\mu\text{-}H)\{\mu_3\text{-}\eta^2\text{-}(\perp)\text{-}C{\equiv}CC_6H_4\text{-}4\text{-}NH_2\}]$ (**2f**); yield: 19.0%, 7.60 mg, yellow solid. IR ν(CO): 2096 (m), 2067 (vs), 2048(vs), 2010(vs) cm^{-1}. *Anal.* Calc. for $C_{17}H_7O_9NRu_3$ (672.45): C, 30.36; H, 1.04; N, 2.08. Found: C, 29.48; H, 1.39: N, 2.30%.

4.4. General procedure for the synthesis of compounds 3a–c

A mixture of $[Ru_3(CO)_{10}(\mu\text{-dppe})]$ (50.0 mg, 0.0510 mmol) and an excess of the corresponding alkyne HC≡CR was refluxed in 30.0 mL of toluene at 90 °C under N_2 for 1 h. The solvent was removed under reduced pressure, and the resulting residue was dissolved in a minimal amount of chloroform and purified by means

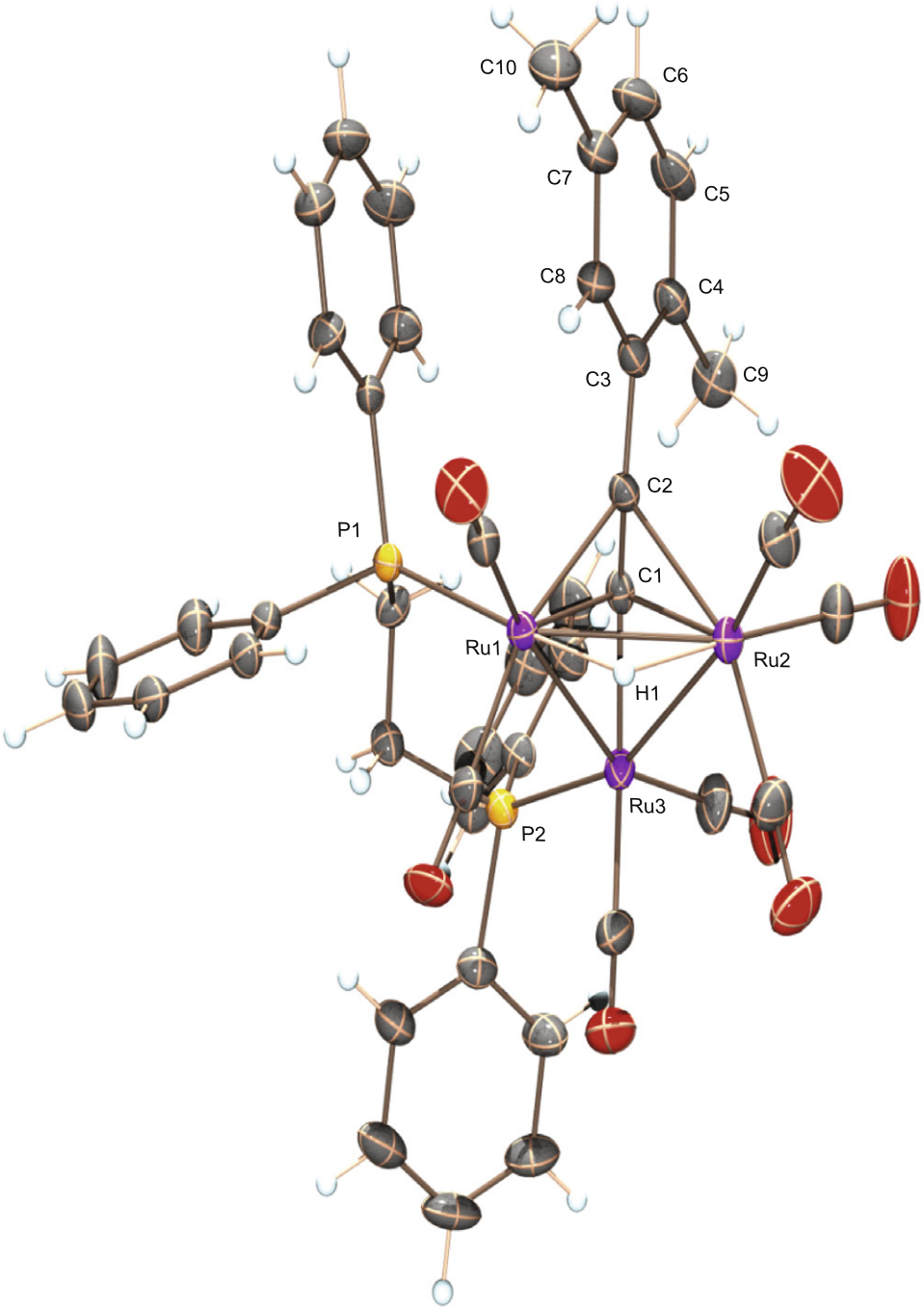

Fig. 4. ORTEP view of compound **3b** (30% probability).

of tlc chromatographic plates [eluent: hexane:CH_2Cl_2 (50:50 v/v)], obtaining the compounds **3a–c** in the first fraction of each reaction.

4.4.1. [$Ru_3(CO)_7$(μ-dppe)(μ-H){μ_3-η^2-(⊥)-C≡C C_6H_4-4-CH_3}] (3a)

1-Ethynyltoluene (18.0 μL, 0.141 mmol). [$Ru_3(CO)_7$(μ-dppe)(μ-H){μ_3-η^2-(⊥)-C≡C C_6H_4-4-CH_3}] (**3a**); yield: 65.0%, 32.5 mg, yellow solid. IR ν(CO): 2059(s), 1998(vs), 1943(m), 1924(sh) cm^{-1}. HR–MS (ESI–TOF); $[M + CO + H_2O]^+$ for ($C_{43}H_{33}O_9P_2Ru_3$) Calc. 1060.8735, found +1060.8759 amu. *Anal.* Calc. for $C_{42}H_{32}O_7P_2Ru_3$ (1013.87): C, 49.76; H, 3.18. Found: C, 49.10; H, 3.27%.

4.4.2. [$Ru_3(CO)_7$(μ-dppe)(μ-H){μ_3-η^2-(⊥)-C≡C C_6H_3-2,5-$(CH_3)_2$}] (3b)

1-Ethynyl-2,5-dimethylbenzene (20.0 μL, 0.140 mmol). [$Ru_3(CO)_7$(μ-dppe)(μ-H){μ_3-η^2-(⊥)-C≡C C_6H_3-2,5-$(CH_3)_2$}] (**3b**);

Table 4
Selected bond lengths (Å) and angles (°) for compounds **2b–d** and **3b**.

Compound	**2b**	**2c$_1$**	**2c$_2$**	**2d**	**3b**
Bond lengths					
Ru(1)–Ru(2)	2.8074(11)	2.7973(3)	2.8007(3)	2.7973(6)	2.8086(7)
Ru(2)–Ru(3)	2.8143(11)	2.7932(3)	2.8016(3)	2.8121(6)	2.7879(7)
Ru(3)–Ru(1)	2.7827(11)	2.8224(3)	2.8158(3)	2.8054(7)	2.8484(6)
C(1)–C(2)	1.292(8)	1.298(4)	1.303(4)	1.303(6)	1.314(8)
C(2)–C(3)	1.470(8)	1.465(4)	1.459(4)	1.486(7)	1.477(6)
Ru(1)–C(1)	2.204(6)	2.196(2)	2.202(2)	2.208(5)	2.214(5)
Ru(1)–C(2)	2.268(6)	2.263(2)	2.265(3)	2.259(4)	2.247(5)
Ru(2)–C(1)	2.202(6)	2.201(2)	2.201(3)	2.199(5)	2.232(6)
Ru(2)–C(2)	2.259(5)	2.306(3)	2.292(3)	2.252(4)	2.282(6)
Ru(3)–C(1)	1.962(7)	1.948(3)	1.952(3)	1.948(4)	1.962(6)
Bond angles					
Ru(1)–Ru(2)–Ru(3)	59.339(17)	60.645(8)	60.345(8)	60.017(15)	61.188(16)
Ru(2)–Ru(3)–Ru(1)	60.21(2)	59.750(8)	59.811(8)	59.729(15)	59.764(16)
Ru(3)–Ru(1)–Ru(2)	60.453(17)	59.605(8)	59.844(8)	60.254(13)	59.048(16)
Ru(3)–C(1)–C(2)	153.9(5)	156.4(2)	155.6(2)	154.1(4)	152.9(4)
C(1)–C(2)–C(3)	145.2(6)	144.9(2)	143.9(3)	140.9(10)[a]	143.6(5)
				147.6(10)[a]	
Interline and interplane angles					
C(1)–C(2)/Ru(1)–Ru(2)	89.75(3)	88.7(2)	89.1(2)	89.94(3)	89.38(3)
C(1)–C(2)/Ru(3)–Ru(2)–Ru(1)	17.94(3)	20.21(2)	19.45(2)	18.08(2)	17.36(3)

[a] Due to positional disorder.

yield: 59.0%, 29.5 mg, yellow solid. IR ν(CO): 2058(s), 2000(vs), 1944(m), 1925(w) cm^{-1}. HR–MS (ESI–TOF); $[M + CO + H_2O]^+$ for ($C_{44}H_{35}O_9P_2Ru_3$) Calc. 1074.8892, found +1074.8898 amu. *Anal.* Calc. for $C_{43}H_{34}O_7P_2Ru_3$ (1027.89): C, 50.25; H, 3.33. Found: C, 49.49; H, 3.26%.

4.4.3. [$Ru_3(CO)_7(\mu$-dppe)(μ-H){μ_3-η^2-(⊥)-C≡CC_6H_2-2,4,5-$(CH_3)_3$}] (3c)

1-Ethynyl-2,4,5-trimethylbenzene (7.40 mg, 0.051 mmol). [$Ru_3(CO)_7$(μ-dppe)(μ-H){μ_3-η^2-(⊥)-C≡CC_6H_2-2,4,5-$(CH_3)_3$}] (**3c**); yield: 62.0%, 31.0 mg, yellow solid. IR ν(CO): 2056(vs), 1992(vs),

Table 5
Crystal data and structure refinement parameters for compounds **2b-d** and **3b**.

Compound	**2b**	**2c**	**2d**	**3b**
Empirical formula	$C_{19}H_{10}O_9Ru_3$	$C_{20}H_{12}O_9Ru_3$	$C_{21}H_{14}O_9Ru_3$	$C_{44}H_{34}C_{13}O_7P_2Ru_3$
Formula weight	685.5	699.51	713.53	1146.21
Crystal colour and shape	red prism	yellow plate	yellow prism	yellow prism
Crystal system	monoclinic	triclinic	tetragonal	triclinic
Crystal size (mm^3)	0.25 × 0.18 × 0.16	0.20 × 0.10 × 0.10	0.35 × 0.29 × 0.5	0.35 × 0.21 × 0.12
Space group	$C2_1/c$	$P\bar{1}$	$I\,4_1/a$	$P\bar{1}$
Unit cell dimensions				
a (Å)	33.888(7)	9.7611(3)	19.907(3)	9.5868(2)
b (Å)	7.7431(15)	14.6946(5)	19.907(3)	12.5022(2)
c (Å)	17.453(4)	17.5227(6)	25.504(5)	20.2746(4)
α (°)	90.00	80.826(3)	90	81.7340(10)
β (°)	90.28(3)	83.974(3)	90	82.4580(10)
γ (°)	90.00	73.633(3)	90	74.5610(10)
V, (Å^3)	4579.53(17)	2375.89(14)	10107(3)	2306.97(8)
Z	8	4	16	2
$D_{calcd.}$ (Mg m^{-3})	1.988	1.956	1.876	1.650
μ, (mm^{-1})	1.998	1.928	1.815	1.260
T (K)	293(2)	293(2)	293(2)	293(2)
λ (Mo K) (Å)	0.71073	0.71073	0.71073	0.71073
Scan type	$\omega-\phi$	$\omega-\phi$	$\omega-\phi$	$\omega-\phi$
2θ range (°)	3.19–27.53	2.92–27.00	2.89–28.88	2.50–27.49
Index ranges				
(*h*min/*h*max, *k*min/*k*max, *l*min/*l*max)	−27/43, −10/9, −20/22	−12/12, −18/18, −22/22	−25/25, −26/22, −32/32	−12/11, −16/15, −26/26
Reflections collected	11847	50279	61484	34554
Independent reflections	5073 (*R*int = 0.0505)	10367 (*R*int = 0.0293)	5908 (*R*int = 0.1979)	10218 (*R*int = 0.0675)
Observed reflections	2734($F > 2\sigma(F)$)	8454 ($F > 2\sigma(F)$)	4171 ($F > 2\sigma(F)$)	6732 ($F > 2\sigma(F)$)
Parameters/restrains	280/0	591/0	374/363	479/0
R final; *R* all data	0.0741, 0.0998	0.0244, 0.0502	0.0479, 0.0851	0.0665, 0.1369
Rw final, *Rw* all data	0.1488, 0.1278[a]	0.0375, 0.0559[b]	0.0873, 0.0992[c]	0.1184, 0.1738[d]
Goodness of fit (GOF) (all data)	0.993	1.109	1.112	1.034
Max, min peaks (e Å^{-3})	0.679/−0.732	0.454/−0.618	0.561/−0.871	1.096/−1.146

Where $P = \sigma(F_o^2 + 2F_c^2)/3$.
[a] $w^{-1} = \sigma^2(F_o^2) + (0.0541P)^2$.
[b] $w^{-1} = \sigma^2(F_o^2) + (0.0244P)^2 + 02314P$.
[c] $w^{-1} = \sigma^2(F_o^2) + (0.0295P)^2 + 12.6554P$.
[d] $w^{-1} = \sigma^2(F_o^2) + (0.0893P)^2 + 2.9746P$.

1942(s), 1923(m) cm^{-1}. HR–MS (ESI–TOF); $[M+H]^+$ for ($C_{44}H_{37}O_7P_2Ru_3$) Calc. 1044.9139, found +1044.9153 amu. *Anal.* Calc. for $C_{44}H_{36}O_7P_2Ru_3$ (1041.92): C, 50.72; H, 3.48. Found: C, 49.99; H, 3.21%.

4.5. General procedure for the synthesis of compounds 4a–c

A mixture of [$Ru_3(CO)_{10}$(μ-dfppe)] (50.0 mg, 0.0370 mmol) and an excess of the corresponding alkyne HC≡CR was refluxed in 20.0 mL of THF at 60 °C under N_2 for 1 h. The solvent was removed under reduced pressure, and the resulting residue was dissolved in a minimal amount of chloroform and separated by means of tlc chromatographic plates [eluent: hexane:CH_2Cl_2 (50:50 v/v)], obtaining the compounds **4a–c** in the second fraction of each reaction. The first fraction corresponds to an unidentified compound.

4.5.1. [$Ru_3(CO)_7$(μ-dfppe)(μ-H){μ_3-η^2-(⊥)-C≡C C_6H_4-4-CH_3}] (4a)

1-Ethynyltoluene (16.0 μL, 0.126 mmol). [$Ru_3(CO)_7$(μ-dfppe)(μ-H){μ_3-η^2-(⊥)-C≡C C_6H_4-4-CH_3}] (**4a**); yield: 63.0%, 31.5 mg, yellow solid. IR ν(CO): 2078(s), 2021(vs), 1997(h), 1976(m), 1951(w) cm^{-1}. HR–MS (ESI–TOF); $[M+H]^+$ for ($C_{42}H_{13}F_{20}O_7P_2Ru_3$) Calc. 1376.6942, found +1376.6950 amu. *Anal.* Calc. for $C_{42}H_{12}O_7F_{20}P_2Ru_3$ (1373.67): C, 36.72; H, 0.88. Found: C, 36.25; H, 0.85%.

4.5.2. [$Ru_3(CO)_7$(μ-dfppe)(μ-H){μ_3-η^2-(⊥)-C≡C C_6H_3-2,5-$(CH_3)_2$}] (4b)

1-Ethynyl-2,5-dimethylbenzene (15.0 μL, 0.105 mmol). [$Ru_3(CO)_7$(μ-dfppe)(μ-H)(μ_3-η^2-(⊥)-C≡C C_6H_3-2,5-$(CH_3)_2$}] (**4b**); yield: 65.0%, 32.5 mg, yellow solid. IR ν(CO): 2073(s), 2014(vs), 1993(sh), 1971(m), 1945(w) cm^{-1}. HR–MS (ESI–TOF); $[M+H]^+$ for ($C_{43}H_{13}F_{20}O_7P_2Ru_3$) Calc. 1388.6953, found +1388.6984 amu. *Anal.* Calc. for $C_{43}H_{14}O_7F_{20}P_2Ru_3$ (1387.69): C, 37.22; H, 1.02. Found: C, 37.46; H, 1.12%.

4.5.3. [$Ru_3(CO)_7$(μ-dfppe)(μ-H)(μ_3-η^2-(⊥)-C≡CC_6H_2-2,4,5-$(CH_3)_3$}] (4c)

1-Ethynyl-2,4,5-trimethylbenzene (8.00 mg, 0.0560 mmol). [$Ru_3(CO)_7$(μ-dfppe)(μ-H)(μ_3-η^2-(⊥)-C≡CC_6H_2-2,4,5-$(CH_3)_3$}] (**4c**); yield: 60.0%, 30.0 mg, orange solid. IR ν(CO): 2075(s), 2017(vs), 1992(sh), 1973(m), 1949(w) cm^{-1}. HR–MS (ESI–TOF); $[M+H]^+$ for ($C_{44}H_{15}F_{20}O_7P_2Ru_3$) Calc. 1402.7109, found +1402.7110 amu. *Anal.* Calc. for $C_{44}H_{16}O_7F_{20}P_2Ru_3$ (1401.72): C, 37.70; H, 1.15. Found: C, 38.96; H, 1.45%.

5. Crystallography

Suitable crystals for compounds **2b–d** and **3b** were obtained by slow evaporation of $CHCl_3$ solution at low temperature (5 °C) for several days. Table 5 shows details for data collection and structure refinement for all compounds. Data for **2b** and **d** and **3b** were collected in an Enraf–Nonius Cappa CCD area detector diffractometer using Mo Kα radiation. The samples were mounted in Micro-Mounts (MiTeGen company) www.mitegen.com. Data collection, determination of unit cell, and integration of frames of all compounds were carried out using the suite COLLECT software [24] and HKL Scalepack [25]. X-ray diffraction data of **2c** were collected on an Oxford Diffraction CCD Gemini diffractometer with graphite-monochromated Mo Kα radiation. Data were integrated, scaled, sorted, and averaged using the CRYSALIS software package [26]. The hydrides in all models were located in their corresponding Fourier maps, and their coordinates and thermal parameters were refined isotropically. The position of the remaining hydrogen atoms the C-bound H-atoms were introduced in calculated positions and refined on their parent atoms. The tert-butyl group in **2d** is disordered over two equally populated positions; the occupancies of the disordered fragments were fixed at 0.5. A semi-empirical absorption correction method (SADABS) [27] was applied in all cases. All structures were resolved by direct methods, completed by subsequent difference Fourier synthesis, and refined by full-matrix least-squares procedures using the SHELX-97 package [27]. All crystallographic programs were used under WINGX program [28].

Acknowledgements

We gratefully acknowledge funding from Consejo Nacional de Ciencia y Tecnología CONACyT, Mexico, (Grants No. CB-106849) and PROMEP, UAEHGO-PTC-258. M.H.S thanks CONACyT for her scholarship. We also wish to thank Yolanda Marmolejo and Ana Lilia Carrasco for their technical assistance to get the elemental analysis of all compounds. Angelica Cerón, Viridiana Juárez and Abril Munguía are gratefully acknowledged for their lab assistance.

Appendix A. Supplementary data

CCDC 847452, 866510, 847463 and 847451 contain the supplementary crystallographic data for **2b–d** and **3b**, respectively. These data can be obtained free of charge via http://www.ccdc.cam.ac.uk/conts/retrieving.html, or from the Cambridge Crystallographic Data Centre, 12 Union Road, Cambridge CB2 1EZ, UK; fax: +44 1223 336 033; or e-mail: deposit@ccdc.cam.ac.uk.

Supplementary data associated with this article can be found, in the online version, at http://dx.doi.org/10.1016/j.poly.2012.10.013.

References

[1] E. Sappa, A. Tiripicchio, P. Braunstein, Chem. Rev. 83 (1983) 203. and references therein cited.
[2] G. Gervasio, D. Marabello, P.J. King, E. Sappa, A. Secco, J. Organomet. Chem. 671 (2003) 137.
[3] E. Sappa, J. Cluster Sci. 5 (1994) 211. and references therein cited.
[4] G.A. Foulds, B.F.G. Johnson, J. Lewis, J. Organomet. Chem. 296 (1985) 147.
[5] D. Roseto, M.D. Vargas, J. Organomet. Chem. 689 (2004) 111.
[6] S. Aime, R. Gobetto, L. Milone, D. Osella, L. Violano, Organometallics 10 (1991) 2854.
[7] P.R. Raithby, M.J. Rosales, in: Adv. Inorg. Chem. Radiochem., vol. 29, Academic Press Inc., 1985, pp. 169–247 and references therein cited.
[8] S. Deabate, R. Giordano, E. Sappa, J. Cluster Sci. 8 (1997) 407–459. and references therein cited.
[9] A.A. Koridze, Russ. Chem. Bull., Int. Ed. 49 (2000) 1135. and references therein cited.
[10] P.R. Raithby, A.L. Johnson, Comprehensive Organometallic Chemistry III, vol. 6, Elsevier, 2007, p. 757. and references therein cited.
[11] E. Sappa, O. Gambino, L. Milone, G. Cetini, J. Organomet. Chem. 39 (1972) 169.
[12] M.J. Morris, in: P. Braunstein, L.A. Oro, P.R. Raith (Eds.), Metal Clusters in Chemistry, vol. I, Wiley-VCH, Germany, 1999, p. 221. and references therein cited.
[13] G. Gervasio, D. Marabello, E. Sappa, A. Secco, J. Organomet. Chem. 690 (2005) 1594.
[14] S. Rivomanana, G. Lavigne, N. Lugan, J.J. Bonnet, Inorg. Chem. 30 (1991) 4110.
[15] S. Rivomanana, C. Mongin, G. Lavigne, Organometallics 15 (1996) 1195.
[16] H. Shen, S.G. Bott, M.G. Richmond, J. Chem. Crystallogr. 27 (1997) 25.
[17] A.J. Deeming, G. Hogarth, M. Lee, M. Saha, S.P. Redmond, H. Phetmung, A.G. Orpen, Inorg. Chim. Acta 309 (2000) 109.
[18] F.J. Zuno-Cruz, A.L. Carrasco, M.J. Rosales-Hoz, Polyhedron 21 (2002) 1105.
[19] M. Hernández-Sandoval, F.J. Zuno-Cruz, M.J. Rosales-Hoz, M.A. Leyva, N. Andrade, V. Salazar, G. Sánchez-Cabrera, J. Organomet. Chem. 696 (2011) 4070.
[20] G. Sánchez-Cabrera, M.A. Leyva, F.J. Zuno-Cruz, M.G. Hernández-Cruz, M.J. Rosales-Hoz, J. Organomet. Chem. 694 (2009) 1949.
[21] M.R. Churchill, F.J. Hollander, J.P. Hutchinson, Inorg. Chem. 16 (1977) 2655.
[22] R.T. Morrison, R.N. Boyd, Organic Chemistry, 6a ed., Prentice-Hall Inc., New Jersey, 1992. pp. 78, 273, 425.
[23] M.I. Bruce, T.W. Hambley, B.K. Nicholson, M.R. Snow, J. Organomet. Chem. 235 (1982) 83.
[24] Nonius, COLLECT., Nonius BV, Delft, The Netherlands, 2001.
[25] Z. Otwinowski, W. Minor, Methods in Enzymology, Academic Press, New York, 1997. pp. 307.
[26] Oxford Diffraction, CRYSALIS software system, version 1.171.33.31., Oxford Diffraction Ltd, Abingdon, UK, 2009.
[27] G.M. Sheldrick, Acta Crystallogr. A64 (2008) 112.
[28] L.J. Farrugia, J. Appl. Crystallogr. 32 (1999) 837.